Journal of Applied Mechanics and Technical Physics, Vol. 38, No. 4, 1997

A MODEL FOR THE FORMATION OF FULLERENES IN CARBON VAPOR

G. I. Sukhinin and O. A. Nerushev

UDC 532.517.4+533.92+546.26

Introduction. The discovery of hollow C_{60} and C_{70} and other fullerenes [1] (a new form of carbon) aroused interest in their properties. The method developed in 1990 for the production of fullerenes in macroscopic quantities by combustion of a graphite arc in atmospheres of noble gases (a so-called fullerene factory) [2] has considerably expanded the possibilities of conducting experiments with fullerenes. It has been shown that fullerenes could hold promise in the production of superconducting materials [3], diamonds, and diamond-like coatings [4]. Furthermore, fullerenes are important for ecological and medicinal applications [5].

On the other hand, the formation of fullerenes (molecules having an extremely high symmetry) from the high-temperature chaos in an electric-arc plasma has not been adequately studied. The high productivity of "fullerene factories" (the yield of fullerenes amounts to 10–15% of the total content of evaporated carbon) requires explanation. It has been established that the fullerene yield depends greatly on the geometrical parameters of reactors and electrodes, on the arc current, and on the composition and pressure of the ambient gas. To determine the optimal conditions of fullerene formation, it is necessary to develop a model that takes into account the processes in the arc, the gas dynamics of the flow of carbon vapor and buffer gas, and the collision kinetics during carbon-cluster formation.

Many papers have been devoted to the kinetics of carbon-cluster formation [6–10]. It has been established [9, 10] that carbon clusters C_k have different spatial structures. However, the modeling of carbon-cluster formation using the Smoluchowski equations has been performed [6–8] ignoring the isomer composition and structure of the clusters.

In this paper, we propose a gas-dynamic and kinetic model for the formation of carbon clusters in a graphite arc (a Kratschmer–Hoffman fullerene factory) burning in a helium or an argon atmosphere. It is shown that carbon vapor issuing from the slot gap between graphite electrodes into a helium (argon) atmosphere forms a turbulent radial jet. The kinetic equation of cluster formation in this jet describes the unsteady clustering of the finite mass of carbon vapor in the heat of the inert gas (Ar or He).

In the paper, we use the Smoluchowski equations, which take into account collisions of clusters of various spatial structures with one another that lead to coagulation. We propose a method which takes into account the spatial structure and rotation of clusters in a first approximation and allows one to determine qualitatively the effectiveness of cross sections of cluster collisions.

The proposed model of carbon cluster formation describes the experimentally observed size distribution of fullerenes and the dependence of the yield of fullerenes on the main determining parameters of a graphite arc reactor.

1. Flow of Carbon Vapor from a Graphite Arc. Figure 1 shows a diagram of a "fullerene factory" using a contact graphite arc [11]. A setup of this type was first used in [2] and then in [12, 13]. The water-cooled cylinder 2, 100 mm in diameter and 150 mm long, is placed inside the vacuum chamber 1 evacuated by a roughing-down pump to 10 Pa. The movable replaceable anode 3 with diameter 6 mm and the expendable cathode 4 with diameter of 10 to 20 mm are located along the cylinder axis. The electrodes are made of pure pyroelectric graphite. The cathode is electrically insulated from the body and fitted with a mechanical seal for translational motion along the axis, and the anode is electrically connected with the chamber.

Kutateladze Institute of Thermal Physics, Siberian Division, Russian Academy of Sciences, Novosibirsk 630090. Translated from Prikladnaya Mekhanika i Tekhnicheskaya Fizika, Vol. 38, No. 4, pp. 140–154, July–August, 1997. Original article submitted October 30, 1995; revision submitted July 5, 1996.

0021-8944/97/3804-0625 $18.00

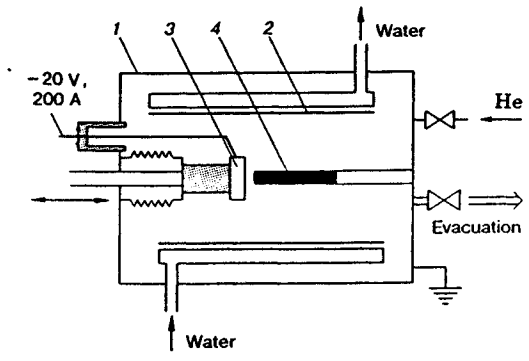

Fig. 1

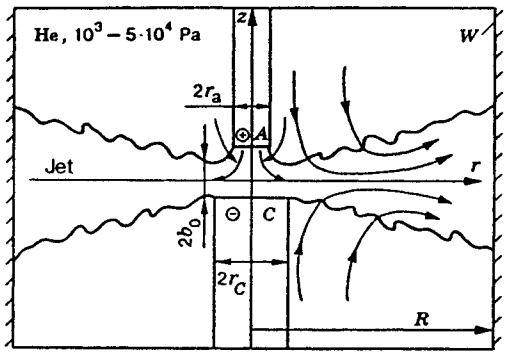

Fig. 2

After preliminary evacuation, the chamber is filled with an inert gas (usually He) to a pressure of the order of 10^3–$5 \cdot 10^4$ Pa. A pressure of $U = 18$–25 V and a current of $I = 100$ A are applied to the electrodes, which initially fit snugly to one another. As the anode burns, the cathode performs longitudinal motion at a rate of about 1 cm/min.

Most of the evaporated graphite in the form of a carbon vapor jet mixed with helium enters the working chamber at a flow rate of the order of 0.01 g/sec, and the remaining part is transferred from the anode to the wider cathode. After turning-off of the voltage, the chamber is cooled and depressurized, carbon black is removed from the walls of the internal cylinder, and the anode is replaced.

During the burning of the arc, the electrode temperature is maintained at 3500 K as a result of intense evaporation of graphite, while the arc temperature can reach 11,000 K [14].

The combustion physics in a high-current arc is extremely complex and includes plasma, gas-dynamic, and radiation processes [13, 14]. No qualitative description of these processes is presently available. It is known, however, that the thermal evaporation of electrodes leads to the formation of a turbulent vapor jet, which interacts with the ambient gas [15, 16]. The gas flow in a high-current arc is determined by the effect of the intrinsic magnetic field. For an extended arc, according to the approximate theory of [16], a limiting velocity is rapidly attained on the axis of the anode jet. This velocity is given by

$$v_a = \left(\frac{\mu_0 I^2}{4\pi S \rho}\right)^{0.5}, \tag{1.1}$$

where I is the arc current, S is the cross-sectional area of the arc, ρ is the density of the ambient gas, and μ_0 is the magnetic permeability of vacuum. For a contact arc, the flow pattern is more complicated because of the interaction between the jet and the electrodes. The gas jet does not have time to reach the limiting velocity because of the narrow electrode gap, and the streamlines turn perpendicular to the arc axis. To determine the flow regime, one can estimate the characteristic Reynolds numbers by using relation (1.1) for the velocity. A Reynolds number higher than 50 was obtained for the flow of a mixture of helium and carbon at a pressure higher than 10^3 Pa, a current of 100 A, and an electrode diameter about 1 cm. As a result, it is concluded that a radial turbulent gas jet is formed which carries the electrode-erosion material.

The qualitative flow pattern in the slotted gap is shown in Fig. 2 (A is the anode, C is the cathode, and W is the water-cooled wall). The carbon concentration in the jet is determined by the pressure of saturated vapors and the electrode temperatures. At $T = 3000$ K, for example, the pressure of saturated carbon vapors above graphite is 100 Pa [17]. The boiling point of graphite is about 4000 K, but, for an arc current of 200 A, the electrode temperature varies from 3400 to 3600 K.

Gas Flow in the Radial Jet from a Contact Arc. We consider a simplified model for the carbon vapor flow in a turbulent radial jet of a carrier gas (He or Ar) assuming that the admixture does not affect the flow structure because of the small carbon concentration. The theory of turbulent jets [18, 19] is largely semiempirical and is based on various assumptions of turbulent mixing or turbulent viscosity. We follow the Görtler theory and apply it to the problem of a radial jet.

We consider a slotted gap having half-width b_0 and radius r_0. Assume that the gas flow is isobaric everywhere beyond the slotted gap. This is supported by the velocity values obtained using formula (1.1): the velocity is subsonic for the given gas composition and temperature. In this case, the gas jet flow is described by the equations of continuity and motion in the boundary-layer approximation:

$$\frac{1}{r}\frac{\partial}{\partial r}(\rho u r) + \frac{\partial}{\partial z}(\rho v) = 0; \tag{1.2}$$

$$\rho u\frac{\partial u}{\partial r} + \rho v\frac{\partial u}{\partial z} = \rho\nu_t\frac{\partial^2 u}{\partial z^2}. \tag{1.3}$$

Here u and v are the radial and axial velocities, ν_t is the turbulent kinematic viscosity, which, according to the Görtler theory, is assumed to be constant at each cross section of the jet: $\nu_t = æ_t b(r)(u_m - u_\infty)$, $b(r) = k_t r$ is the thickness of the jet mixing zone, u_m is the maximum flow velocity on the jet axis, $u_\infty = 0$ is the minimum velocity on the jet boundary or the velocity of the cocurrent flow (for the buoyant jet, $u_\infty = 0$), and $æ_t$ and k_t are empirical constants.

We assume that the gas flow is incompressible (the limitation of this assumption is considered below). Then, system (1.2) and (1.3) can be solved by introducing the stream function Ψ:

$$ur = u_0 r_0\frac{\partial\Psi}{\partial z}, \qquad vr = -u_0 r_0\frac{\partial\Psi}{\partial r}. \tag{1.4}$$

In this case, the continuity equation (1.2) is fulfilled automatically. The solution of Eq. (1.3) will be sought in self-similar form by introducing the coordinates r and $\varphi = \sigma z/r$ (σ is a constant that characterizes the jet divergence). The introduction of the self-similar variables is equivalent to considering an effective point source with a given momentum flux in the plane of jet propagation. As usual, for the radial velocity we assume [19] that

$$ur = u_0 r_0 F'(\varphi), \qquad F'(0) = 1 \tag{1.5}$$

(the prime denotes differentiation with respect to the self-similar variable φ). Hence,

$$\Psi = \int_0^\infty ur\,dz = \frac{u_0 r_0 r}{\sigma}F(\varphi). \tag{1.6}$$

Then, for the axial velocity v we have

$$vr = \frac{u_0 r_0}{\sigma}(F'(\varphi) - F), \qquad F(0) = 1. \tag{1.7}$$

From the constancy of the momentum flux through the jet cross section including the initial section at the slot exit,

$$2\pi\rho\int_0^\infty u^2 r\,dz = 2\pi\frac{(u_0 r_0)^2}{\sigma}\rho\int_0^\infty (F'(\varphi))^2\,d\varphi = 2\pi b_0 r_0\rho V^2,$$

where $V = v(r_a)$ is the radial gas velocity, we find that the quantity u_0 does not depend on r, and the radial velocity of the radial jet in the plane $z = 0$ is given by

$$u_m(r) = \frac{u_0 r_0}{r} \qquad \left(u_0 = V\sqrt{\frac{3b_0\sigma}{2r_0}}\right). \tag{1.8}$$

Thus, the maximum (over the cross section) velocity of the radial jet varies in inverse proportion to the distance from the source

Substituting (1.5) and (1.7) into the equation of motion (1.3), we have

$$F'^2 + FF'' + (æ_t k_t\sigma^2)F''' = 0. \tag{1.9}$$

Choosing the unknown constant σ from the condition $\sigma^2 = 1/(2æ_t k_t)$ and integrating (1.9) subject to the

boundary condition $F''(\varphi = 0) = 0$, we obtain the equation

$$2FF' = F'', \tag{1.9'}$$

which has a solution

$$F(\varphi) = \tanh\varphi. \tag{1.10}$$

Finally, for the velocities u and v from relations (1.5), (1.7), and (1.10) we obtain the self-similar solution

$$u = \frac{u_0 r_0}{r}(1 - \tanh^2\varphi); \tag{1.11}$$

$$v = \frac{u_0 r_0}{r\sigma}((1 - \tanh^2\varphi)\varphi - \tanh\varphi). \tag{1.12}$$

According to the experimental data, the single empirical constant of the theory is $\sigma \approx 8.3$, which corresponds to an angle of 6°, for which the radial velocity reaches half its maximum value on the axis.

Kinetic Equation for Carbon Clusters in the Radial Jet. We study the motion of clusters in the gas flow. Because of the electrode erosion, a certain amount of carbon atoms and ions enters the gas jet issuing from the electrode gap. At temperatures corresponding to the electrode temperatures, the degree of ionization is small and, with distance from the arc axis, it decreases further as a result of recombination. Association of atomic particles to form carbon molecules C_2, C_3, etc., i.e., carbon clusters, begins even in the electrode gap. For the steady flow beyond the electrode gap, this process can be described by the following system of continuity equations for clusters of any size:

$$\operatorname{div}(n_k V_k) = \sum_j^{k_m} K_{k-j,j} n_{k-j} n_j - \sum_j^{\infty} K_{kj} n_k n_j - K_{kk} n_k^2 = \tilde{G}_k. \tag{1.13}$$

Here n_k is the number density of k-mers, V_k is their velocity, which includes the averaged gas-flow velocity and the diffusion velocity of k-mers, K_{ij} is the constant of formation of an $(i+j)$-mer upon collision of an i-mer and a j-mer, $k_m = k/2$ for even k and $k_m = (k-1)/2$ for odd k, the first term on the right side of the equation describes the formation of a k-mer from smaller clusters, the second term is the incorporation of k-mers into clusters of larger sizes upon their collision with clusters of size j, and the last term takes into account that collision of two k-mers leads to the death of each of these and to the formation of one $2k$-mer. Relation (1.13) does not contain terms responsible for monomolecular decay of the clusters formed. This means that, in the presence of a large number of internal degrees of freedom, the bond energy released upon cluster coagulation is distributed among different modes, and the cluster is then thermalized in collisions with the buffer gas. Furthermore, the experiments of Hunter et al. [9] showed that carbon clusters of various structures do not break up during scattering by gas targets even at relative energies of the order of 100–150 eV.

The kinetic operator $\tilde{G}_k$ satisfies the obvious relation

$$\sum_k k\tilde{G}_k = 0, \tag{1.14}$$

which reflects the conservation of the total mass of carbon clusters. The total number of carbon atoms at a certain point of the jet r, z is

$$n_C(r, z) = \sum_k k n_k(r, z). \tag{1.15}$$

We consider the left side of Eq. (1.13). For a turbulent jet, molecular diffusion can be ignored. For a radial jet in the boundary-layer approximation, in which the turbulent diffusion across the jet is much larger than the longitudinal diffusion, Eq. (1.13) has the form

$$\frac{1}{r}\frac{\partial}{\partial r}(n_k u r) + \frac{\partial}{\partial z}(n_k v) = \tilde{G}_k + \nu_D \frac{\partial^2 n_k}{\partial z^2}, \tag{1.16}$$

where $\nu_D = æ_D b(r) u_m$ is the coefficient of turbulent diffusion, and the coefficient $b(r) = k_t r$, as well as ν_t, is

constant across the jet. Multiplying Eq. (1.16) by k and summing up all k with allowance for the continuity equation (1.2), we obtain

$$u\frac{\partial}{\partial r}(n_C) + v\frac{\partial}{\partial z}(n_C) = \nu_D\frac{\partial^2 n_C}{\partial z^2}. \tag{1.17}$$

As for the flow velocities u and v, we shall seek a solution to the equation of the concentration field (1.17) in self-similar form

$$n_C(r,z) = n_C(r,\varphi) = \frac{N_0 r_0}{r}\Theta(\varphi), \qquad \varphi = \frac{\sigma r}{z}. \tag{1.18}$$

Substituting this relation into (1.17) and using relations (1.5) and (1.7) for the velocities u and v, for $\Theta(\varphi)$ we write

$$2\Theta F + \delta\Theta' = 0, \qquad \delta = \frac{æ_D}{æ_t}. \tag{1.19}$$

Here δ is the Schmidt turbulent number, which depends on the flow type; we assume that $\delta = 1$ (for an axisymmetric gas jet, $\delta \approx 0.75$). Then, with allowance for relation (1.9′), Eq. (1.19) becomes

$$\delta(\Theta'/\Theta) = F''/F', \qquad \Theta(\varphi) = (F'(\varphi))^{1/\delta}. \tag{1.20}$$

Thus, in the turbulent radial jet, the distribution profile of a small additive behaves similarly to the profile of the radial velocity of the flow. The condition of conservation of carbon mass flow leads to

$$2\pi\int_0^\infty u n_C r\,dz = 2\pi\frac{N_0 u_0 r_0^2}{\sigma}\int_0^\infty (F'(\varphi))^2\,d\varphi = 2\pi b_0 r_0 N_C V,$$

where N_C is the number density of carbon atoms at the slot exit and $N_0 = N_C\sqrt{3b_0\sigma/(2r_0)}$.

Note that for excess temperatures $(T - T_\infty)$ in the radial jet, we can obtain a solution similar to the solution for the carbon additive concentration (1.18):

$$\frac{T - T_\infty}{T_0 - T_\infty} \approx \frac{r_0}{r}. \tag{1.18′}$$

To study further the kinetic equation (1.16), we introduce the relative size distribution of clusters:

$$c_k = \frac{n_k}{n_C}, \qquad \sum_k k c_k = 1. \tag{1.21}$$

We use the following strong but reasonable assumption: because of the turbulent mixing across the jet, the relative concentrations depend only on the longitudinal coordinate r. With allowance for the relations for the velocities u and v and for the carbon density n_C, the kinetic equation (1.16) for the dimensionless concentration, subject to the boundary conditions $c_k = c_k^0$ for $r = r_0$, takes the simple form

$$\frac{dc_k}{dr/r_0} = \frac{N_C r_0}{V}\Big(\sum_{j=1}^{k_m} K_{k-j,j}c_{k-j}c_j - \sum_{j=1}^{\infty} K_{kj}c_k c_j - K_{kk}c_k^2\Big). \tag{1.22}$$

Below, we shall assume that $c_1^0 = 1$ and $c_k^0 = 0$ for all the remaining k.

Equation (1.22) describes cluster formation in radial jets. It can be extended, however, to a fairly wide class of quasi-one-dimensional flows:

$$\frac{dc_k}{dr/r_0} = \frac{n_C(r)r_0}{u(r)}\Big(\sum_{j=1}^{k_m} K_{k-j,j}c_{k-j}c_j - \sum_{j=1}^{\infty} K_{kj}c_k c_j - K_{kk}c_k^2\Big). \tag{1.22′}$$

Here, the ratio of the local density of carbon $n_C(r)$ to the carrier gas velocity $u(r)$ is used instead of the constant parameter N_C/V for a radial turbulent jet. For a wide class of flows, this ratio has the form

$$\frac{n_C(r)}{u(r)} = \frac{n_C(r_0)}{u(r_0)}\left(\frac{r}{r_0}\right)^{-\eta},$$

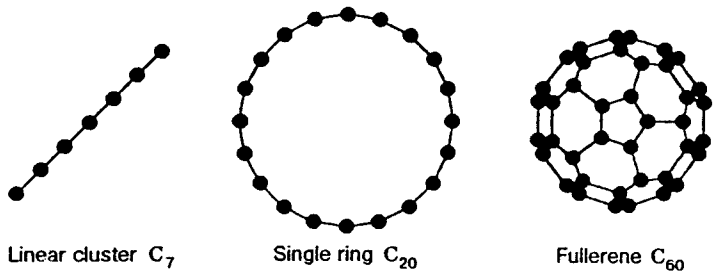

Fig. 3

where η is an empirical parameter that depends on the type of flow.

2. **Choice of Rate Constant for Carbon-Cluster Formation.** To solve the kinetic equations (1.22) and (1.22′), it is necessary to know the rate constants of cluster formation K_{ij}. Note that, at present, theoretically founded rate constants are not available, and, furthermore, the mechanism of cluster formation has not yet been understood. One of the widely used assumptions of fullerene formation by evaporation of large fragments of graphite planes followed by the formation a polyhedron was disproved experimentally [20]. It was shown that with evaporation of an electrode made of graphite sections of pure carbon C^{12} and ^{13}, the resulting fullerenes had a mixed isotope composition that corresponded to the complete mixing of atoms in the electrode gap. This is only possible when the initial state of the condensed vapor is monoatomic.

It was established [10] that carbon clusters exist in the form of several groups of spatial (structural) isomers, which are linear chains, single rings and polyrings (plane structures), and spherical hollow fullerenes. Figure 3 shows the qualitative structure of some of these formations. With the same number of atoms, clusters k can take different shapes, i.e., they can break into groups of structural isomers [10]. In addition, each structural group can consist of a large number of isomers that differ in shape, number of atomic bonds, number of dangling bonds, degree of vibrational excitation of numerous vibratory states, etc. All these parameters affect the cross sections of cluster collisions with each other and with atoms of the ambient gas, the reactivity of clusters, velocities of intermolecular transitions, or decay velocities of clusters during collisions.

A simple and clear model for the formation of carbon clusters is required. In our opinion, this model should be based on features of the cluster structure, which allow one to describe correctly cluster collisions with each other and also the reactivity of clusters, which depends greatly on their structure, degree of excitation, gas temperature, etc. Precisely this reactivity ultimately determines the fine structure (magic numbers) of the size distribution of clusters.

In this paper, we propose a simple model for collisions of carbon clusters. According to [9, 10], clusters C_k are linear chains for $k < 10$, monocycles for $10 < k < 50$, binary cycles for $k \geqslant 20$, ternary cycles for $k \geqslant 30$, and fullerenes for $k > 30$. The cross sections of their collisions are studied using the classical approach. We assume that the diameter of the carbon atom is $d_C = 0.155$, and the length of the C–C bond is $l_C = 0.14$ nm. In this case, the gas-kinetic cross section for collisions of carbon monomers is $\sigma_{11} = \pi d_C^2 = 0.0754$ nm^2.

In the gas phase, the clusters move at thermal velocity, colliding with atoms of the ambient gas and with each other, and rotate. We assume that the rotational degrees of freedom of the clusters are in equilibrium with the translational degrees of freedom of the clusters and the carrier gas.

The cross sections for collisions of clusters C_k with He atoms were determined by von Helden et al. [10] from mobility measurements, and they agree well with the results obtained by the Monte Carlo method. In the calculation it was assumed that helium and carbon atoms are hard spheres. The orientations of clusters of different shapes relative to the motion of helium atoms were averaged. The data of [10] for the cross sections of collisions of helium atoms with linear and circular clusters and also with hollow fullerenes are shown in Fig. 4 by curves 1–3. In addition, the figure shows the data of our calculations for hypothetical compact clusters with close packing (curve 4) and for collisions of circular clusters (curve 5) and fullerenes with monomers C (curve 6). For atoms and small clusters, collision-free flight through cyclic clusters is possible. Helium atoms "see" a small vicinity of the perimeter of linear and cyclic carbon clusters. This is responsible for the linear

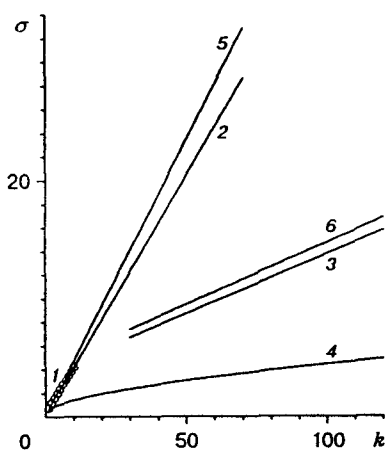

Fig. 4

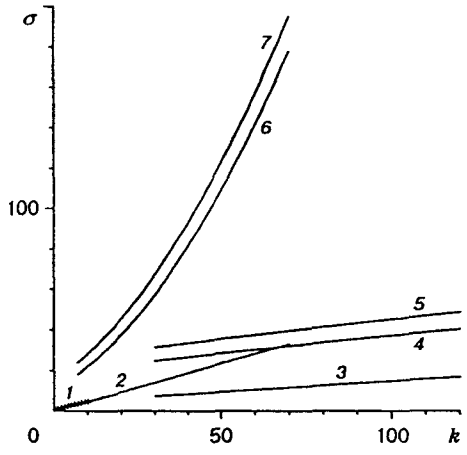

Fig. 5

dependences of the cross sections of $He + C_k$ collisions on k. The linearity of the cross section of collisions of He with spherical hollow fullerenes is explained by the fact that carbon atoms are located only on the fullerene surface, so that the cross section increases linearly with increase in k. The cross sections of collisions of carbon clusters with carbon monomers C differ insignificantly from the cross section of collisions with helium atoms and vary linearly with increase in k.

To describe the interactions of fullerenes with one another, one should study collisions of noncompact structures with one another. The collision cross sections for fullerenes, which are compact spherical particles, are determined fairly simply. For fullerene C_{60}, the radius at which the carbon atoms are located is $r_{60} = 0.355$ nm. Hence, the gas-kinetic cross section is

$$\pi R_{60}^2 = \pi(r_{60} + d_C/2)^2 = 7.79\sigma_{11} = 0.5877 \text{ nm}^2.$$

For the other fullerenes, using the results of [10], we can obtain the semiempirical relation

$$\pi R_k^2 = \pi(r_k + d_C/2)^2 = (3.71 + 0.101k)\sigma_{11},$$

i.e., the gas-kinetic cross section for fullerenes varies linearly with change of its number.

A more complicated situation arises for collisions of linear clusters (chains) and cycles. Linear and plane clusters are in rotational motion. During the time of flight τ of cluster C_i past cluster C_j, the linear cluster with size i is able to rotate through angle α_i. Estimation shows that

$$\tau = 2(R_i + R_j)/\langle v_{ij}\rangle = 2((R_i + R_j)/\langle v_C\rangle)(ij/(i+j))^{1/2}, \qquad \alpha_i = \tau\omega_i,$$

where $\omega_i = (2\langle E_r\rangle/J_i)^{1/2}$ is the angular velocity of rotation of the ith cluster, $\langle v_{ij}\rangle$ is the average relative velocity of the clusters, R_i and R_j are the radii of the carbon clusters, which depend on the mass number and isomer structure of the clusters, $\langle E_r\rangle \sim kT$ is the average rotational energy of the cluster, and $J_i \approx M_C l_C^2 i^3/12$ is the characteristic moment of inertia of the cluster. As a result, for linear and cyclic clusters, we obtain $\alpha \geqslant \pi/2$.

Thus, to calculate collisions of a linear cluster, we use the effective cross section of a freely oriented disk or of a sector with angle α and with radius determined by the linear size of the chain. Similar calculations for circular and polycyclic clusters showed that, because of rotation, clusters, except for monomers, cannot pass by them without collision. Therefore, circular and polycyclic clusters collide as spherical particles.

In this paper, for paired collisions of a carbon i-mer with a j-mer we use the cross sections $\sigma_{ij} = \pi(R_i + R_j)^2$ referred to the collision cross section of monomers σ_{11}. Figure 5 shows some cross sections for collisions of carbon clusters of various structures with a monomer C (curves 1–3), a single ring C_{20} (curves 5, 7), and a fullerene C_{60} (curves 4 and 6) related to the collision cross section of carbon monomers: curve 1 refers to $C + C_k$ (linear clusters), curve 2 to $C + C_k$ (single rings), curve 3 refers to $C + C_k$ (fullerenes), curve 4

to $C_{60} + C_k$ (fullerenes), curve 5 to $C_{20} + C_k$ (fullerenes), curve 6 to $C_{60} + C_k$ (rings), and curve 7 to $C_{20} + C_k$ (rings).

The above results are approximate. To determine more accurately collision cross sections for carbon clusters, one should calculate collisions by the Monte Carlo method using averaging over orientations and rotational velocities of clusters and taking into account the isomer structure of polycycles, the difference of their shape from regular circles, and vibrational excitation. Nevertheless, this would not change the following main conclusions:

(a) the effective cross sections for collisions of carbon atoms with clusters C_k of any radius vary linearly with increase in k but at different velocities for linear, plane, and spherical clusters;

(b) the effective cross sections for collisions of linear and plane clusters C_k with one another bear a quadratic relationship to k;

(c) the effective cross sections for collision of fullerenes C_k vary linearly with k.

Thus, carbon clusters differ significantly from clusters of metals or noble gases, which have compact structures and whose collision cross sections depend on k as $k^{2/3}$ (curve 4 in Fig. 4). As is shown below, precisely the nonmonotonic complex dependence of the cross sections of collisions of carbon clusters with one another is responsible for the experimentally observed features of size distribution of the clusters.

The rate constants for collisions K_{ij} have the form

$$K_{ij} = v_C \sqrt{(i+j)/ij}\,\sigma_{ij} P_{ij}, \tag{2.1}$$

where $v_C = (8k_B T/\pi M_C)^{-1/2}$ is the thermal velocity of carbon atoms, M_C is the mass of a carbon atom, and P_{ij} is the probability of formation of a cluster with size $(i+j)$ upon collision of an i-mer with a j-mer.

The reactivities P_{ij} require special study using the methods of quantum chemistry. It is necessary to take into account the isomer structure of the clusters, the number of saturated and dangling bonds, the vibrational and electron states, the formation of an intermediate complex and its stabilization in collisions with the carrier gas (which takes the heat of the reaction), and intramolecular transitions, which lead to the formation of new bonds, etc. Solution of this problem is presently unrealizable and is not the goal of this paper (Bernholc and Phillips [6] studied the reactivities for small clusters in the Polányi–Brönsted approximation, and Creasy [7] performed a phenomenological account of stabilizing collisions with a carrier gas). Below we shall restrict ourselves to only simple approximations.

Obviously, at high temperatures ($T \geqslant 3000$ K) in a dense gas, the probabilities $P_{ij}(T)$ are fairly low and decrease with further rise in temperature. This statement follows immediately from the law of acting masses, because the equilibrium in this case is shifted toward dissociation products [21]. In the region of $T \sim 3000$–1000 K, the probabilities $P_{ij}(T)$, varying slowly, reach a maximum value and, with further decrease in temperature, they decrease again.

In this paper, we assume that $P_{ij} = 1$ for all i and j that are not equal to 60 and 70 and for some other stable fullerenes. For the indicated i and j, the probabilities are considered constant ($P_{ij} < 1$). A comparison with the experimental data made it possible to find the empirical value of $P_{i,60}$. In some cases for small unstable fullerenes, the probabilities P_{ij} were specified differently for even and odd numbers i and j, and this led to alternation of even and odd clusters C_k for $k \geqslant 30$, as observed in experiments.

3. Kinetic Equations. Equations (1.22) do not take into account the isomer composition of clusters. The concentration c_k is the overall (for all isomers) fraction of clusters composed of k atoms. For simplicity, we assumed the existence of only two types of clusters, single rings and fullerenes with more than 30 atoms per cluster, and the collision cross sections were chosen according to the experimental data of [10].

The stationary continuity equation (1.22) in this form is completely equivalent to the nonstationary kinetic equation with the dimensionless time x. Numerical solution of Eq. (1.22) involved no difficulties. We used an implicit solution scheme in which some terms on the right side of the kinetic equations were taken from the previous "time" layer. The calculations were performed in the range of $1 < x < 2500$ with steps $\Delta x = 0.05$ or 0.1. A check of the difference of the sum $\sum_k k c_k$ from unity at each step with the subsequent correction of all the occupancies c_k showed that the chosen system was stable, and the calculation error did

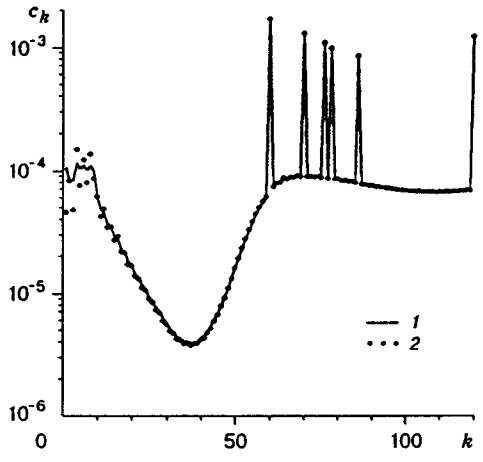

Fig. 6

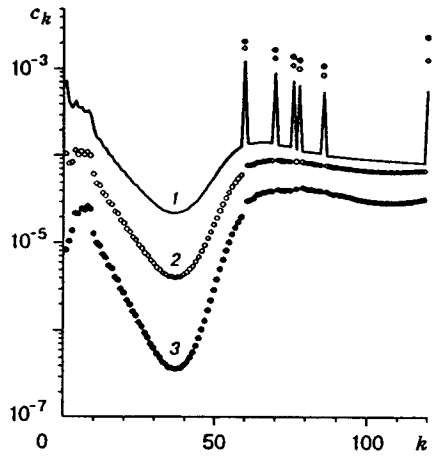

Fig. 7

not exceed fractions of a percent for any k. The solution was sought for mass numbers k from 1 to 120, so that the occupancy was, in essence, the total occupancy of clusters whose sizes are equal to or larger than 120. The test solution of the system with cross sections for compact clusters tends to the well-known log-normal relations of [22].

Figure 6 shows two initial size distribution of clusters at distance $x = 50$. The first distribution corresponds to the case where only carbon monomers ($c_1^0 = 1$, $c_k^0 = 0$ for $k > 1$) issue from the electrode gap, and the second distribution corresponds to the case where half of the carbon atoms are initially in the form of dimers C_2 ($c_1^0 = 0.5$, $c_2^0 = 0.25$, $c_k^0 = 0$ for $k > 2$). It is evident that the mass spectra depend markedly on the initial distribution only for values of k of the order of 10–15. For larger values of k, the distributions practically coincide. This indicates that, in the given formulation, the initial distribution is relatively insignificant for the size distribution of large clusters.

The variation in the size-distribution function for clusters is given in Fig. 7 (curves 1–3 correspond to the dimensionless distances $X = 25$, 50, and 100, respectively. Evidently, in the range from 20 to 40, a characteristic dip occurs which is due to large collision cross sections of cyclic clusters. Small clusters that enter this range of sizes pass it rapidly, supplementing the cluster distribution in the fullerene range. The distribution function becomes nonmonotonic. With increase in distance, the fraction of small clusters decreases, whereas, in the second wide maximum located behind the dip, the fraction of clusters increases. Against the background of this nonmonotonic distribution function for relatively stable fullerenes C_{60}, C_{70}, C_{76}, C_{78}, etc., pronounced peaks occur, which grow with increase in distance from the source.

The main goal of the operation of a "fullerene factory" is to produce fullerenes C_{60}, C_{70}, etc. Therefore, an important characteristic is $Y_k(X) = kc_k(X)$, which is the yield of clusters of the given size k ($X = AR_C/r_0$, where R_C is the radius of the reactor).

Figure 8 shows the dependence of the yield Y_{60} of fullerenes C_{60} on the distances X for various values of the parameter $P = P_{60,i}$. For $P = 0$ (curve 1), monotonic growth of the fullerene yield with increase in X is observed. In this case, the fullerene yield tends asymptotically to ~0.26. Peaks that correspond to other stable fullerenes behave similarly. Curve 1 shows that the maximum value of the achievable yield of fullerenes C_{60} with the given cluster distribution is $Y_{60}^{\max} \approx 0.26$. More accurate allowance for the isomer structure and a certain variation in the cross sections of collisions of clusters with one another do not lead to a marked change in the quantity $Y_{60}^{\max}$, which is independent of the type of cross section and depends only on the collisional constants K_{ij}. Even the monomolecular decay of the resulting clusters has an effect not on $Y_{60}^{\max}$, but only on the rate of attainment of the asymptotic value.

The dependence for Y_{60} at $P = 1$ is shown by curve 2. The yield of k-mers at distance X_k reaches a maximum value $Y_k^{\max}$ and then decreases monotonically. The value of $Y_{60}^{\max}$ in this case is considerably smaller than the experimental values.

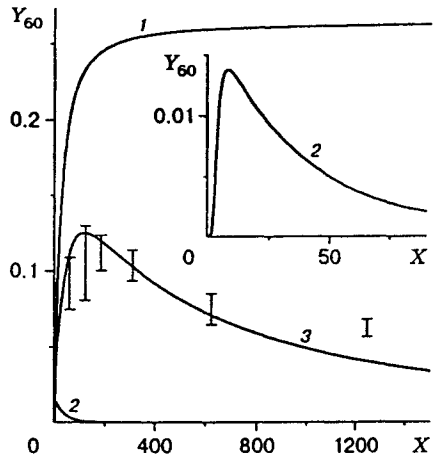

Fig. 8

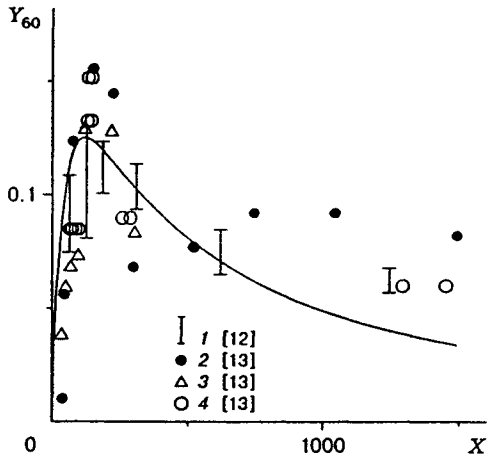

Fig. 9

Curve 3 illustrates the yield of fullerenes C_{60} for the intermediate value of the parameters $P = 0.2$. In this case, $Y_{60}^{\max} = 0.12$ for $X_{60} \approx 125$, and then it decreases slowly because of the growth of unstable clusters of C_{60} to larger sizes. The fullerene yields obtained are optimal for the majority of setups of such type. The vertical curves in this graph correspond to the experimental data of [12].

Under the assumptions used above, the dimensionless coordinate x is related to the radial coordinate via the initial coordinates, velocity, and concentrations. For real setups, the boundary radial coordinate R_C is determined by the position of the chamber wall or the black-collecting shield, and the variation of the upper boundary of integration X with the x coordinate is related to the variation in the operating parameters.

We write the expression for the boundary coordinate X as

$$X = \frac{n_0 v_C \sigma_{11} R_C}{u_0} = \frac{Q}{m_C} \frac{\langle P \rangle}{\chi^2} \frac{v_C \sigma_{11}}{\mu_0 I^2} \frac{p \mu_g}{RT} \frac{\pi R_C r_0}{b_0},$$

where Q is the carbon mass flow rate, σ_{11} is the collision cross section for monomers, p is the pressure of the buffer gas, μ_g is the mole mass of the buffer gas, and R is the universal gas constant. The velocity of the gas jet at the exit from the electrode gap is assumed to be proportional to the axial velocity in the anode arc: $u_0 = \chi v_a$ (χ is a modeling parameter). As is shown below, the value of the parameter $\langle P \rangle / \chi^2$ is close to unity.

The experimental results of [12] for the dependences of the yield of fullerenes C_{60} on pressure and on the type of buffer gas, shown in Fig. 8, agree qualitatively with the solution of (1.22) for $P_{i,60} = 0.2$ (curve 3). Figure 9 shows the fullerene yield for $P_{i,60} = 0.2$ versus helium pressure (points 1 and 2), arc current (points 3), and electrode gap (points 4). The calculation results (curve) agree well with experimental data (vertical lines).

4. Conclusions. The results obtained in Sec. 3 show that the proposed gas-dynamic model for the flow of a mixture of a buffer gas with carbon vapors from a contact graphite arc (a turbulent radial jet) and the kinetic model of carbon cluster formation in collisions with each other describe qualitatively the size distribution of the clusters. A nonmonotonic distribution function holds for relatively small distances from the source ($x = 5$–25). For clusters with $k \sim 20$–40, a characteristic dip occurs, which is due to the anomalously high effective gas-kinetic sections of linear and cyclic clusters. Precisely gas-dynamic sections, determined by the large cross section of cyclic clusters being in rotational motion, lead to the high frequency of collisions of relatively large clusters with one another. The model takes into account the birth of clusters of definite sizes with coagulation of smaller clusters and allows one to compare the local production of given species, for example, fullerenes C_{60}, by various bimolecular pathways. In this case, the dependence of the probability of coagulation on the cluster size is not significant.

We consider in detail processes that lead to the formation of C_{60}. The first sum on the right side of Eq. (1.22) for the C_{60} production contains 30 members, which describe the frequencies of $C_i + C_{60-i}$ collisions.

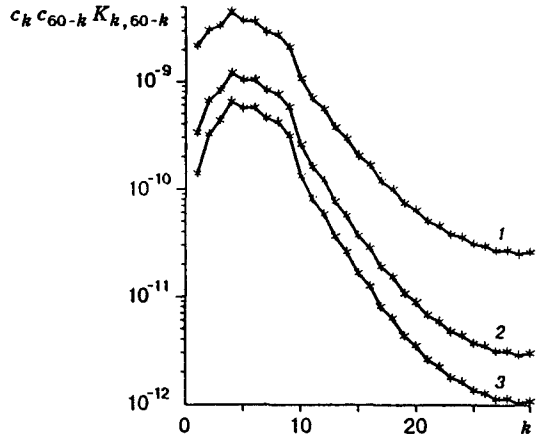

Fig. 10

Figure 10 gives the rates of this reaction at three different points of the flow for the same conditions as the size spectra in Fig. 7. The considerable difference in cross section (see Figs. 4 and 5) is responsible for the nonmonotonic distribution function (see Figs. 6 and 7) and for the considerable difference in frequency between the collision reactions. Noteworthy is the predominance of coagulation reactions of small clusters over coagulation reactions of "halves" with close sizes. This is due to both the sudden decrease in their concentration (see Fig. 7) and the presence of the relative particle velocity, which is small for collisions of two large clusters, in relation (2.1) for the reaction constants. Thus, even ignoring the higher reactivity of linear clusters compared with rings and fullerenes, we obtain predominance of reaction pathways occurring by the addition of small (< 10) clusters. The differences in relative reactivities obtained in [6, 8] lead to some differences of the distribution functions from the functions that follow from the collision characteristics of molecules.

The experimental dependence of the fullerene yield on the gas pressure [13] shows a maximum that is absent in both the theoretical dependence and in the experimental data of [12]. This can be explained by the change in the flow gas-dynamics due to the transition from the radial flow to upward convective flow, which is not taken into account in the model. The difference between the experimental data of [12] and [13] can be attributed to the marked difference in dimensions between the reactors used and to the different spatial arrangement of electrodes in the reactors.

We give an estimate of the region in which convective processes should be taken into account. We write the following equation for the vertical velocity component in a turbulent jet:

$$\rho u \frac{\partial v}{\partial r} + \rho v \frac{\partial v}{\partial z} = \rho \nu_t \frac{\partial^2 v}{\partial z^2} - \rho g \frac{T - T_\infty}{T_\infty}. \tag{4.1}$$

Here T is the gas temperature in the jet and T_∞ is the temperature of the ambient gas. System (1.2), (1.3), and (4.1) should be supplemented by an equation for the temperature with boundary conditions at the electrodes and water-cooled surfaces of the reactor. The excess temperature $(T - T_\infty)$ varies slowly along the jet because of turbulent mixing (1.18′). We consider Eq. (4.1) on the axis of the radial jet and compare the first term on its left side with the last term of the right side taking into account relations (1.8) and (1.18′) for the excess temperature and radial velocity. Introducing the "convective" radius r_C, for which the radial velocity $u(r_C)$ is compared with the cross velocity $v(r_C)$, we obtain

$$r_C = u_0 \left(\frac{T_\infty r_0}{(T_0 - T_\infty) g} \right)^{1/2}.$$

At distances larger than r_C, the streamlines of the radial jet are curved, and the jet begins to float up with a certain convective velocity, while the process of turbulent diffusion continues. The kinetics of cluster formation

is still described by Eq. (1.22′), but with the parameter $\eta = 1$. Thus, in the range $r > r_0$, all cluster formation processes depend on $\ln(x)$ rather than on the distance x itself. The value of r_C depends on the specific features of the reactor (mainly on its geometric dimensions). With change in the flow regimes, the fullerene yield is determined by the convective radius rather than by the wall radius.

Because of turbulent and convective processes and unsteady initial conditions, the radial flow studied in this paper can become unsteady and break up into a number of individual jets. Each of the jets can be imagined as axisymmetric turbulent flow. The integral carbon flow rate from the source remains unchanged. The initial jet velocities are given by relation (1.1). The dependences of the axial velocity and the vapor density on the coordinate along the jet axis coincide with similar dependences on the radial coordinate for radial flow (1.11) and (1.18). The kinetic equations (1.22) also remain unchanged. The results given in Figs. 6–10 hold true for this flow as well.

In the above calculations, we did not consider the difference in reactivity between the clusters and processes that occur after collisions of clusters with one another (stabilization of the resulting clusters with their structural rearrangement, annealing, and elimination of excitation by the buffer gas). These processes are taken into account implicitly in the model by the assumptions that the lifetime of metastable conglomerates of carbon is fairly large in the range studied (because of the large number of internal degrees of freedom) and that the cross sections and frequencies of collisions with the buffer gas are large.

The phenomenological model presented describes well the general view of mass spectra and yield of fullerenes, but does not explain the character of alternation of even and odd clusters in the mass spectra. This alternation can be explained by allowing for the reactivities of clusters using additional experimental data or by calculating reactivities for all types of isomers of even and odd clusters. Inclusion of the reactivities in Eqs. (1.22) and (1.22′) will not complicate calculations.

We would like to thank S. A. Novopashin for fruitful discussions of the formulation of the problem and N. I. Yavorskii for discussions of the gas-dynamic aspects of the problem.

This work was supported by the International Science Foundation (Grant No. RPN000), The International Science Foundation and the Russian Government (Grant No. RP000), and the Russian Foundation for Fundamental Research (Grant No. 96-03-33770a).

REFERENCES

1. H. W. Kroto, J. R. Heath, S. C. O'Brien, et al., "C_{60}-buckminsterfullerene," *Nature*, **318**. 162–163 (1985).
2. W. Krätschmer, L. D. Lamb, K. Fostiropulos, et al., "Solid C_{60}: a new form of carbon," *Nature*, **347**, 354–358 (1990).
3. V. M. Loktev, "Doped fullerite, the first three-dimensional organic superconductor," *Fiz. Nizkikh Temp.*, **18**, No. 3, 217–233 (1992).
4. T. Sekine, "Diamond recovered from shocked fullerites," *Proc. Jpn. Acad. Ser. B*, **68**, 95–99 (1992).
5. R. Dagani, "Biological studies of unsubstituted C_{60} launched," *Chem. Eng. News*, **72**, No. 24, 7–8 (1994).
6. J. Bernholc and J. C. Phillips, "Kinetics of cluster formation in the laser vaporization source: carbon clusters," *J. Chem. Phys.* **85**, 3258–3267 (1986).
7. W. R. Creasy, "Some model calculations of carbon cluster growth kinetics," *J. Chem. Phys.* **92**, 7223–7233 (1990).
8. V. A. Schweigert, A. L. Aleksandrov, Yu. N. Morokov, and V. M. Bedanov, "MINDO/3 study of the interactions of small carbon clusters," *Chem. Phys. Lett.*, **235**, 221–229 (1995).
9. J. M. Hunter, J. L. Fye, E. J. Roskamp, et al., "Annealing carbon cluster ions: a mechanism for fullerene synthesis," *J. Phys. Chem.* **98**, 1810–1818 (1994).
10. G. von Helden, Hsu Ming-Teh, P. R. Kemper, M. T. Bowers, "Structures of carbon cluster ions from 3 to 60 atoms: linears to rings to fullerenes," *J. Phys. Chem.* **95**, 3835–3837 (1991).

11. V. A. Mal'tsev, O. A. Nerushev, S. A. Novopashin, et al., "Polarization of fullerenes," *Pis'ma Zh. Éksp. Teor. Fiz.*, No. 10, 634–637 (1993).
12. Y. Saito, M. Inagaki, Y. Shinohara, et al., "Yield of fullerenes generated by contact arc method under He and Ar: dependence on gas pressure," *Chem. Phys. Lett.*, **200**, 643–648 (1992).
13. D. Afanas'ev, I. Blinov, F. Bogdanov, et al., "Fullerene formation in arc discharge," *Zh. Tekh. Fiz.*, **64**, No. 10, 76–90 (1994).
14. W. Finkelnburg and H. Maecker, "Elektrische boeden und thermisches plasma," *Handbuch der Physik*, 1956, **22**, 254–444 (1956).
15. G. R. Jones and M. T. C. Fang, "The physics of high power arc," *Rep. Prog. Phys.*, **43**, 1415–1464 (1980).
16. S. Ramakrishnan, A. D. Stokes, and J. J. Lowke, "An approximate model for high-current free-burning arc," *J. Phys. D: Appl. Phys.*, **11**, 2267–2280 (1978).
17. S. Dushman, *Scientific Foundations of Vacuum Technique*, John Wiley and Sons, New York (1962).
18. G. N. Abramovich (ed.), *Theory of Turbulent Jets* [in Russian], Nauka, Moscow (1984).
19. Dr. H. von Schlichting, *Grenzschict-Theorie*, Verlag G. Braun, Karlsruhe (1964).
20. G. Meijer and D. S. Bethune, "Laser deposition of carbon clusters on surfaces A new approach to the study of fullerenes," *J. Chem. Phys.*, **93**, 7800 (1990).
21. L. D. Landau and E. M. Lifshits, *Statistical Physics* [in Russian], Nauka, Moscow (1976).
22. M. Villarica, M. J. Casey, J. Goodisman, and J. Chaiken, "Application of fractals and kinetic equations to cluster formation," *J. Phys. Chem.*, 98, 4610–4625 (1993).